Available online at http://docs.lib.purdue.edu/jate

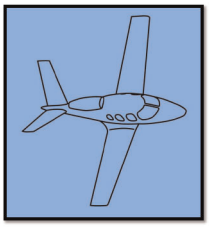

JATE

Journal of Aviation Technology and Engineering 12:1 (2023) 64–72

A New Empirical Law for the Prediction of the Zero-Lift Pitching Moment Coefficient of Swept and Tapered Wings

Mondher Yahyaoui

Ecole d'aviation de Borj El Amri, Tunisia

Abstract

A new empirical law for the prediction of the zero-lift pitching moment coefficient of trapezoidal wings with linear twist and constant taper and sweep in subsonic flow is introduced. This law is quite general in that it does not rely on the use of charts and spans the normal range of values of taper ratio, aspect ratio, and sweep for subsonic aircraft. It does not, however, accommodate different airfoils along the wingspan and only positive sweep has been considered. The empirical law was first derived for the incompressible regime and then an additional empirical law for the compressibility effect has been provided. The results compare favorably with experimental data for straight wings and with some pre-existing empirical methods for wings with low to moderate sweep. It is also shown that the most widely used method of estimating the zero-lift pitching moment coefficient is highly inaccurate.

Keywords: pitching moment coefficient, empirical law, swept wings, vortex-lattice method, Göthert's rule

List of Symbols

A: aspect ratio
a_0: section lift-curve slope
a_H: horizontal tail lift-curve slope
b: span
c: chord
c_o: central chord
$C_{m_{ac}}$: wing's moment coefficient at the aerodynamic center
$c_{m_{ac}}$: section's moment coefficient at the aerodynamic center
i_H: horizontal tail's angle of incidence
K_M: compressibility correction factor
V_H: horizontal tail volume ratio
α: angle of attack of airplane's longitudinal axis
β: subsonic compressibility parameter
δ_E: elevator deflection angle

http://dx.doi.org/10.7771/2159-6670.1252

ε_0: average downwash angle on horizontal tail at zero lift
η_H: $\bar{q}_{\infty H}/\bar{q}_{\infty}$
θ: washout angle
λ: taper ratio
Λ: wing sweep at quarter chord

Introduction

The pitching moment coefficient is an important parameter in the analysis of an airplane's longitudinal stability. In steady flight for instance and in the linear range of variation of the pitching moment coefficient, it can be expressed as (Roskam, 1979)

$$C_m = C_{m_0} + C_{m_\alpha}\alpha + \frac{\partial C_m}{\partial i_H} i_H + \frac{\partial C_m}{\partial \delta_E}\delta_E \qquad (1)$$

where C_{m_0} is the pitching moment coefficient for $\alpha = i_H = \delta_E = 0$:

$$C_{m_0} = C_{m_{ac_{wb}}} + C_{L_{0_{wb}}}(\bar{x} - \bar{x}_{ac_{wb}}) + \eta_H a_H V_H \varepsilon_0 + C_{m_p} \qquad (2)$$

where C_{m_p} represents the contribution of the propulsion system to the pitching moment coefficient. $C_{m_{ac_{wb}}}$ and $C_{L_{0_{wb}}}$ are the pitching moment coefficient at the aerodynamic center and the lift coefficient at zero angle of attack of the wing–body combination, respectively. Following Multhopp (1942), the pitching moment coefficient of the wing–body combination is often written as

$$C_{m_{ac_{wb}}} = C_{m_{ac_w}} + \Delta C_{m_{ac_b}} \qquad (3)$$

where $\Delta C_{m_{ac_b}}$ is the contribution of the fuselage to C_{m_0}, while $C_{m_{ac_w}}$ is the pitching moment coefficient at the aerodynamic center of the wing, which is the subject of the present work.

A new empirical law for the estimation of this coefficient is introduced. The data needed for the development of this law are based on numerical values obtained using a well-tested cambered VLM code developed by the author (Author, 2014; Author, 2019a, 2019b). The vortex-lattice numerical method is a singularity method which has been around for many decades and is well documented in the literature (Bertin & Smith, 1998). The accuracy of our numerical values will be demonstrated by comparing to some experimental data.

It will be clearly shown that most of the main pre-existing methods used to predict such an important parameter generally have an essential drawback to them. One of these methods involves a semiempirical equation (Abbott & Von Doenhoff, 1959; Anderson, 1936) based on lifting line theory. It relies on the use of charts which makes it less convenient for computer programming. The second method involves an empirical equation (Kapteyn, 1972) based on lifting surface theory and is summarized in Torenbeek (1982). It is more or less accurate for straight wings but seems to lose accuracy for wing sweep angles larger than 20°. It does not rely on the use of charts which makes it convenient for computer programming. Both of these methods are limited to the incompressible flight regime only.

The third method is the widely referenced semiempirical law from the USAF-DATCOM (Finck, 1978). It relies on the use of charts and these are given for taper ratios of 0, 0.5, and 1 only. It will be clearly shown that this method is highly inaccurate.

The new empirical law introduced in the present work is good for trapezoidal wings with linear twist and constant taper and sweep. It does not, however, accommodate the case of wings with varying airfoil along the span and only positive sweep was considered. The main law was developed for the incompressible regime, and then an additional empirical equation for the effect of compressibility was also provided. The method does not rely on the use of charts, which makes it convenient for computer programming.

Details of the New Empirical Law

By definition, the pitching moment coefficient at the aerodynamic center is independent of the angle of attack. Hence, it was evaluated numerically by computing the pitching moment coefficient $C_m(x)$ at different chordwise locations of the pitch axis, for two different values of the angle of attack, and finding the intersection of the two straight lines as in Figure 1.

The database needed for the establishment of the new law was generated by computing $C_{m_{ac}}$ for a wide range of values of the aspect ratio, taper ratio, and sweep angle. The new empirical equation was found to be of the same general form as the pre-existing empirical or semiempirical ones (Anderson, 1936; Finck, 1978; Kapteyn, 1972), i.e.,

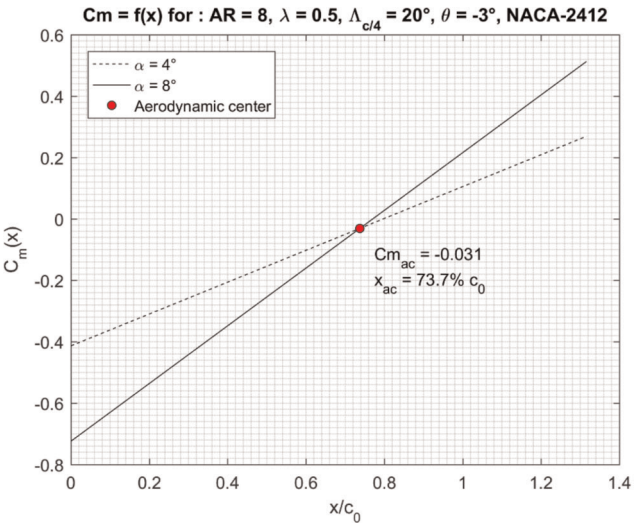

Figure 1. An example of finding a wing's $C_{m_{ac}}$: $A = 8$, $\lambda = 0.5$, $\theta = -3°$, $\Lambda = 20°$, and NACA 2412.

$$C_{m_{ac}} = K_0 c_{m_{ac}} + K_\theta \theta \tag{4}$$

where $c_{m_{ac}}$ is the airfoil's pitching moment coefficient at the aerodynamic center. Our computations confirm the linear variation of $C_{m_{ac}}$ with the twist angle θ as in Figure 2. Considering equation (4), numerical values for K_0 were obtained by computing $C_{m_{ac}}$ for zero twist and dividing it by the airfoil's pitching moment coefficient:

$$K_0 = \frac{C_{m_{ac}}|_{\theta=0}}{c_{m_{ac}}} \tag{5}$$

This was done for taper ratios of 0.2, 0.3, 0.4, 0.5, 0.6, 0.8, and 1 and aspect ratios of 4, 6, 7, 8, and 10. In order to generate numerical values for K_θ, the same wing geometric configurations computed with zero twist are recomputed for $\theta = -3^\circ$. The choice of this value of the twist angle is arbitrary in view of the linear variation of $C_{m_{ac}}$ with θ. The values for $C_{m_{ac}}$ were used as follows:

$$K_\theta = \frac{C_{m_{ac}} - C_{m_{ac}}|_{\theta=0}}{\theta} \tag{6}$$

We will begin here by giving the final equations making up the new empirical law. Some of the details behind these equations will be given once all the elements have been defined.

Coefficient K_0 is of the form

$$K_0 = c_1 \left[1 - c_\lambda \left(\frac{\Lambda}{50}\right)^n\right] \tag{7}$$

with Λ in degrees. Constant c_1 is given by

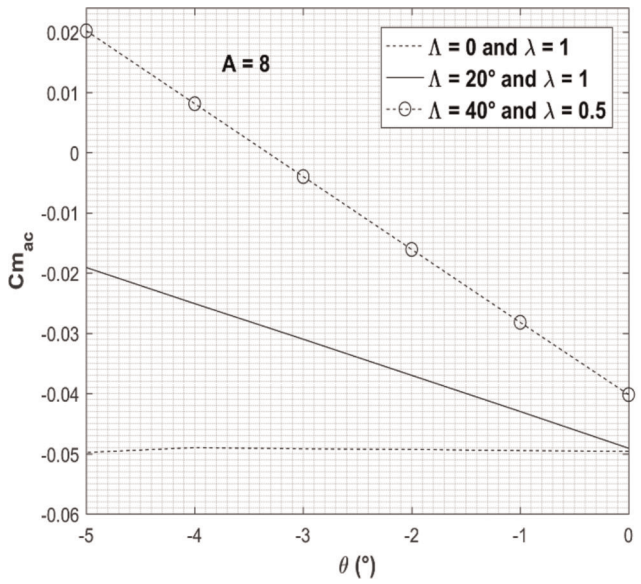

Figure 2. Linear variation of wing pitching moment coefficient with the twist angle.

$$c_1 = a_1 - 0.0037|10 - A|^{n_1} \tag{8}$$

with

$$a_1 = 1.124 - 0.086(1-\lambda)^{4.1}\lambda^{0.25} \tag{9}$$

$$n_1 = 1.59 + 0.4(1-\lambda)^{4.1} \tag{10}$$

Constant c_λ in equation (7) is given by

$$c_\lambda = 0.26 + 0.1(1-\lambda)^2 \tag{11}$$

while exponent n is given by

$$n = K_{A_1} - K_{A_2}(1-\lambda)^{4.8}\lambda^{0.032A} \tag{12}$$

with

$$K_{A_1} = 3.07 - 0.1483(A-4) \tag{13}$$

$$K_{A_2} = 0.06 + 0.3233(A-4) \tag{14}$$

Coefficient K_θ in equation (4) is given by

$$K_\theta = -a_2\left[(\sin\Lambda)^{0.78} + 0.9\Lambda^{1.75}\right] \tag{15}$$

with Λ in radians, and

$$a_2 = K_{A_3} - K_{A_4}(1-\lambda)^{5.5}\lambda^{0.02A} \tag{16}$$

$$K_{A_3} = 0.0037 + 0.0018(A-4) \tag{17}$$

$$K_{A_4} = 0.0013 + 0.0020(A-4) \tag{18}$$

Equations (4) and (7)–(18) define our new law for the estimation of the zero-lift pitching moment coefficient of trapezoidal wings with linear twist and constant sweep and taper, in the incompressible regime. An empirical equation for the compressibility effect on this coefficient will also be provided.

Steps for Finding K_0

Our general approach to defining the parameters in equations (7)–(18) was to plot the discrete numerical values for each parameter and then, by trial and error and an educated guess of basic mathematical functions, fit a curve to these numerical values. The process was rather lengthy and we will spare the reader some of the details.

Defining coefficient K_0 involved finding the equations for the three parameters c_1, c_λ, and n in equation (7). For a given taper ratio and for each value of the aspect ratio we found by trial and error numerical values for these three parameters. Sample results are shown in Figure 3 for a taper ratio $\lambda = 0.5$. The discontinuous lines represent equation (7) once numerical values of c_1, c_λ, and n have been found, while the markers represent the VLM

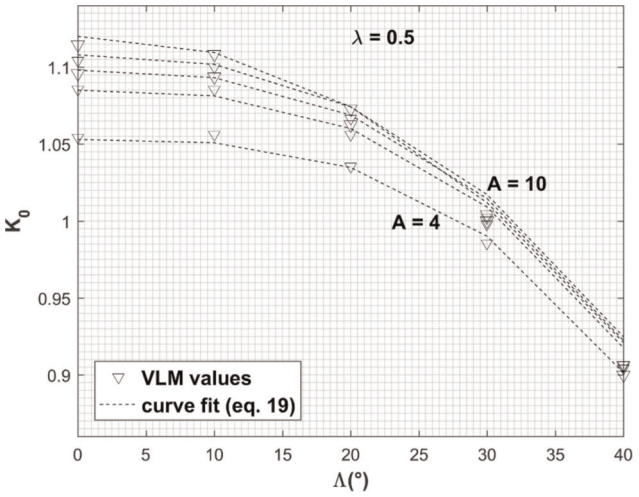

Figure 3. Curve-fit (equations (19)) to VLM values of K_0: $\lambda = 0.5$ and $A = 4$, 6, 7, 8, and 10.

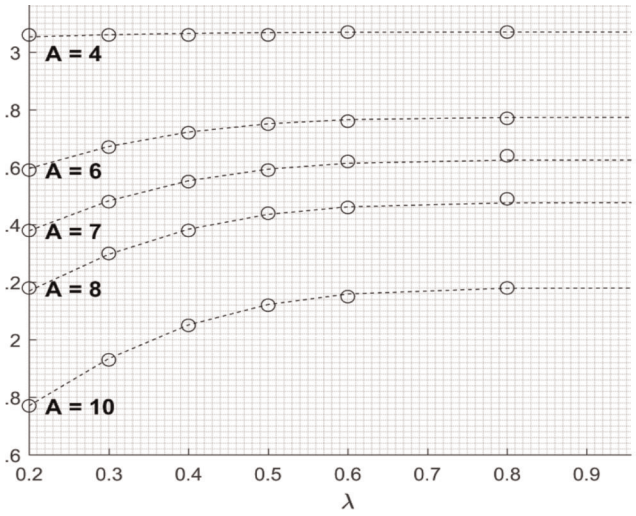

Figure 4. Agreement between equation (12) and the discrete values of exponent *n*.

numerical values obtained using equation (5). The curve-fit equations for this value of the taper ratio are

$$\begin{aligned} K_{04} &= 1.053\left[1-0.285(\Lambda/50)^{3.06}\right] \\ K_{06} &= 1.085\left[1-0.285(\Lambda/50)^{2.75}\right] \\ K_{07} &= 1.098\left[1-0.285(\Lambda/50)^{2.59}\right] \\ K_{08} &= 1.108\left[1-0.285(\Lambda/50)^{2.44}\right] \\ K_{010} &= 1.12\left[1-0.285(\Lambda/50)^{2.12}\right] \end{aligned} \tag{19}$$

The subindexes of K_0 are the values of the aspect ratio.

Equations similar to (19) were obtained for all the other taper ratios and the maximum discrepancy between the curve-fit equations and the numerical values for all the cases was less than 1.5% up to a sweep angle of 30° and a maximum of 2.3% at a 40° sweep angle. We therefore had numerical values for c_1, c_λ, and n at all the values of A and λ considered in this study. These were used to define empirical equations for all three parameters.

First, we fitted the curve given by equation (8) to c_1 and, in the process, we had to introduce two new parameters a_1 and n_1 whose curve fits are equations (9) and (10). Then we had to find an equation for c_λ. This parameter is a function of taper ratio only and the process led toequation (11).

The final step in defining K_0 was to find an equation for exponent n in equation (7). This was a lot more complicated since this parameter is a function of both A and λ. First of all, the discrete values of n were plotted as functions of λ for every value of the aspect ratio. Then we had to devise functions which would fit the different sets of discrete values of n. The process led to equation (12). Parameter K_{A_1} was assigned the maximum of the discrete values of n for each value of A and these correspond to $\lambda = 1$ as indicated by Figure 4. We were able to fit a straight line to the numerical values of K_{A_1} whose equation is (13). Then we subtracted the proper function of λ and A which would allow for a close match with the discrete values of n. It was found by trial and error that the function that needed to be subtracted from K_{A_1} is of the form of the last term in equation (12), i.e.,

$$K_{A_2}(1-\lambda)^{4.8}\lambda^{0.032A}$$

Having found a curve fit for every set of values of n corresponding to a different value of aspect ratio as in Figure 4, we obtained the numerical values necessary to define parameter K_{A_2} which is function of aspect ratio alone. It was then found that K_{A_2} also fits to a straight line whose equation is (14).

Steps for Finding K_θ

We started by plotting values of K_θ obtained using equation (6) as a function of the sweep angle for a given taper ratio and different values of the aspect ratio. The trial-and-error process of trying to fit curves to the datasets converged on equation (15). This is illustrated in Figure 5 for a taper ratio of 0.3. The curve-fit equations for this particular value of the taper ratio are

$$\begin{aligned} K_{\theta 4} &= -0.0035\left[(\sin\Lambda)^{0.78}+0.9\Lambda^{1.75}\right] \\ K_{\theta 6} &= -0.0067\left[(\sin\Lambda)^{0.78}+0.9\Lambda^{1.75}\right] \\ K_{\theta 7} &= -0.0082\left[(\sin\Lambda)^{0.78}+0.9\Lambda^{1.75}\right] \\ K_{\theta 8} &= -0.0098\left[(\sin\Lambda)^{0.78}+0.9\Lambda^{1.75}\right] \\ K_{\theta 10} &= -0.0130\left[(\sin\Lambda)^{0.78}+0.9\Lambda^{1.75}\right] \end{aligned} \tag{20}$$

The numerical values of the parameter in equation (15) were then plotted as functions of taper ratio for fixed values

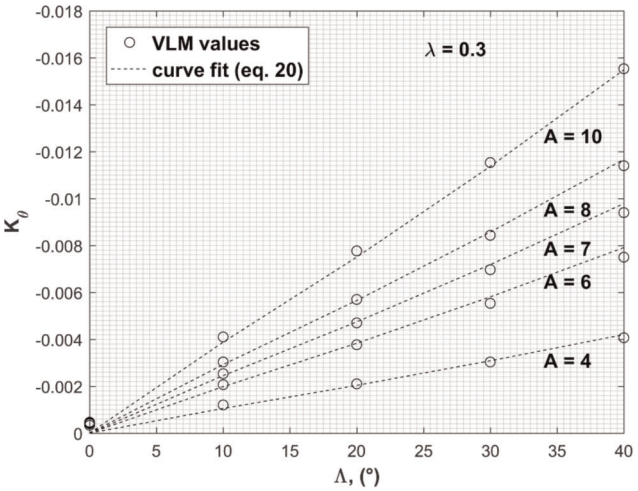

Figure 5. Curve fit to the numerical values of K_θ for $\lambda = 0.3$ and different values of aspect ratio (equations (20)).

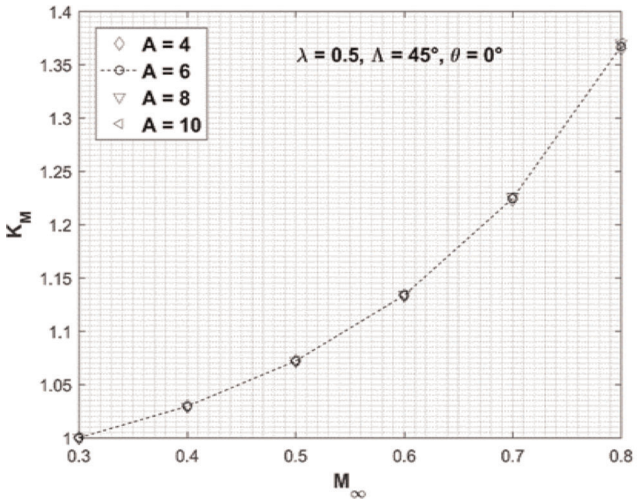

Figure 7. Effect of aspect ratio on the compressibility correction factor K_M.

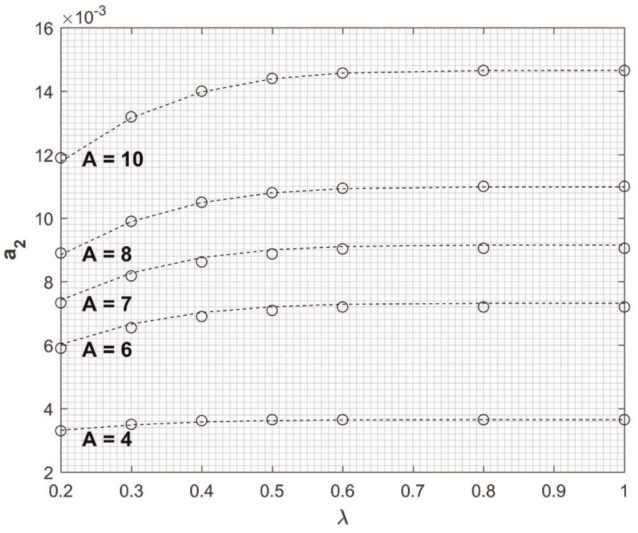

Figure 6. Agreement of equation (16) with the discrete values of coefficient a_2.

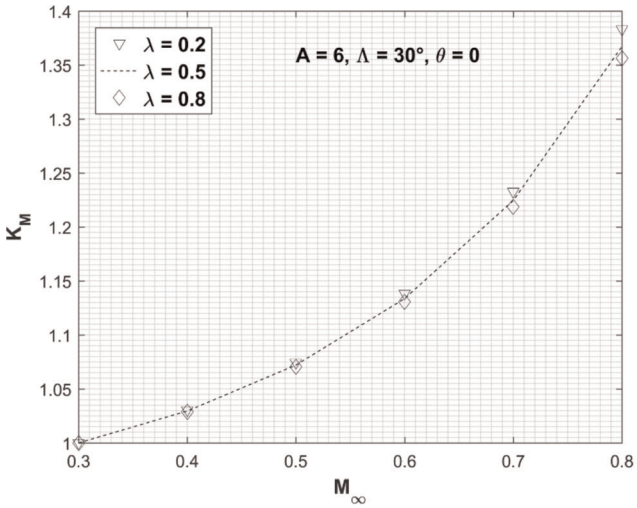

Figure 8. Effect of taper ratio on the compressibility correction factor K_M.

of aspect ratio. It was noted that this constant followed the same overall trend as that of exponent n given by equation (12). Therefore, we only had to adjust the exponents of λ and $(1–\lambda)$ and establish the right equations for coefficients K_{A_3} and K_{A_4} in equation (16). The process led to the empirical equations (16)–(18). The close agreement between equation (16) and the discrete values of a_2 is illustrated in Figure 6.

Compressibility Correction

Compressibility effects on $C_{m_{ac}}$ were investigated using Göthert's rule (Shapiro, 1952). The effect of compressibility on the pitching moment coefficient is represented by a factor K_M such that

$$C_{m_{ac}} = K_M C_{m_{ac_0}} \tag{21}$$

where $C_{m_{ac_0}}$ is the incompressible value of the pitching moment coefficient. As shown in Figures 7 and 8, K_M is practically independent of aspect ratio and varies very slightly with taper ratio. However, as indicated by Figure 9, this factor is a function of the sweep angle. This contradicts the chart in the USAF-DATCOM document (Finck, 1978) which gives one curve for K_M regardless of sweep or any other geometric parameter.

Once again, by trial and error, we were able to fit the following empirical equation to the numerical values of K_M for the different values of the sweep angle:

$$K_M = 1 + c_\Lambda M_\infty^{3.3} \tag{22}$$

$$c_\Lambda = 1.15\left[1 - 0.55\left(\frac{\Lambda}{50}\right)^{1.8}\right] \tag{23}$$

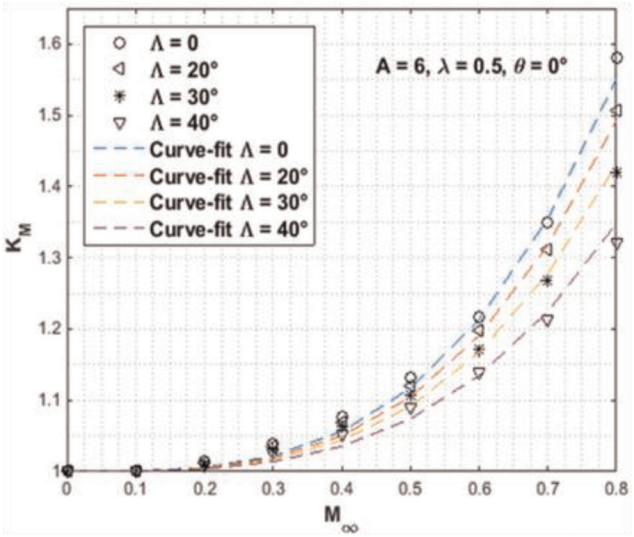

Figure 9. Empirical equation (22) versus VLM values of K_M.

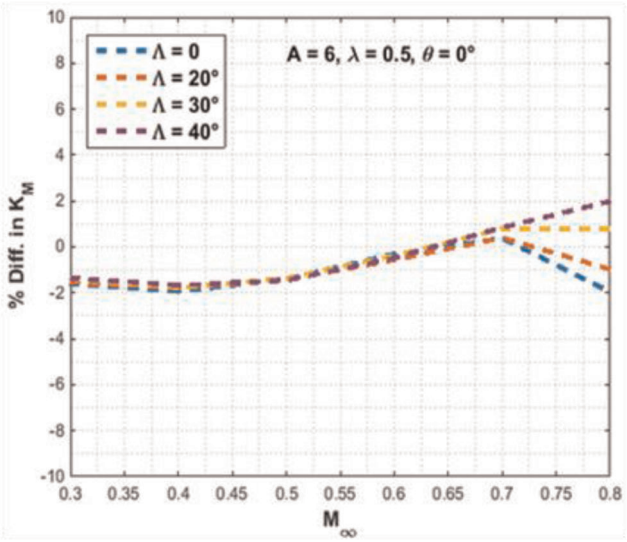

Figure 10. Percent differences in K_M values between equation (22) and numerical values.

where Λ is in degrees. Curves corresponding to equation (22) are plotted in Figure 9 along with the numerical values of K_M. The agreement is quite good since the relative difference is less than 2% as indicated by Figure 10.

Results and Discussion

The new empirical law gives results which are in close agreement with the numerical values of $C_{m_{ac}}$. Sample cases are shown in Figure 11 for a taper ratio $\lambda = 0.4$. The agreement is satisfactory for this case as well as for the other values of taper ratio considered in this study. The airfoil used is the NACA 2412 and its pitching moment coefficient was taken to be equal to -0.047.

We also checked the accuracy of equation (4) to values of aspect ratio outside the range of values used in this study. Cases of aspect ratio lower than 4 and higher than 10 are given in Table 1. The agreement between the VLM numerical values and those given by equation (4) is satisfactory as indicated by the percent differences.

Validation of the Results in the Incompressible Regime

Two experimental values available for comparison correspond to wings with the following geometric properties (Neely et al., 1947):

- $A = 8$, $\lambda = 0.4$, $\theta = -4.5°$, and $\Lambda = 0$. The root side airfoil is the NACA 4416 and the tip side airfoil is the NACA 4412. The experimental value for $C_{m_{ac}}$ is -0.099. The value given by the new empirical law using the NACA 4415 airfoil is -0.103. The relative difference is 4%.
- $A = 8$, $\lambda = 2/7$, $\theta = -3°$, $\Lambda = 0$, and the NACA 44-series airfoil with a thickness ratio of 14.7%. The experimental value for $C_{m_{ac}}$ is -0.097. Our new empirical law using the NACA 4415 airfoil gives a value of -0.102. The relative difference is 5%.

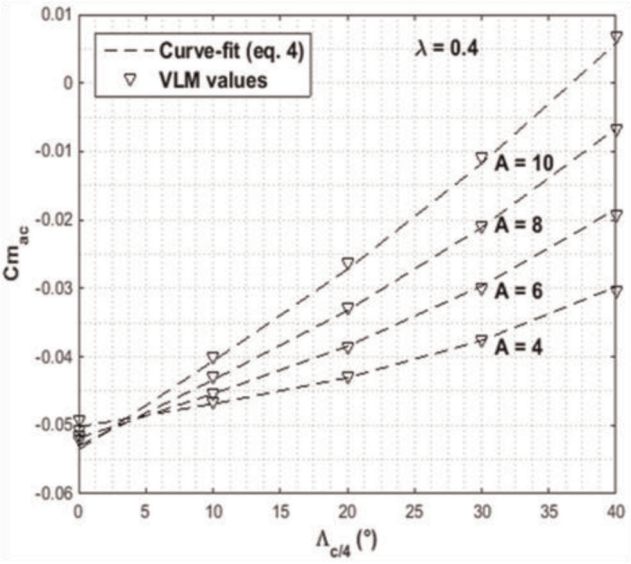

Figure 11. Example of agreement between equation (4) and VLM values of $C_{m_{ac}}$.

Our new empirical law was also compared to some pre-existing methods. The first is Anderson's equation (Anderson, 1936; given in detail in Abbott & Von Doenhoff, 1959):

$$C_{m_{ac}} = EC'_{m_{ac}} - \left(\frac{G}{E} a_0 A \tan \Lambda_{ac}\right)\theta \qquad (24)$$

where E and G are determined from charts. For this method,

$$K_0 = E \qquad (25)$$

Table 1
Equation (4) tested outside the range of values of aspect ratio used in this study ($\theta = -3^\circ$, NACA 2412).

Wing geometry	VLM	Equation (4)	Difference
$A = 3$, $\lambda = 0.3$, $\Lambda = 35^\circ$	−0.0372	−0.0368	1.1%
$A = 3.6$, $\lambda = 0.4$, $\Lambda = 27^\circ$	−0.0403	−0.0398	1.2%
$A = 11$, $\lambda = 0.5$, $\Lambda = 25^\circ$	−0.0138	−0.0140	1.4%
$A = 12$, $\lambda = 0.5$, $\Lambda = 0^\circ$	−0.0525	−0.0521	0.8%

$$K_\theta = -\frac{G}{E} a_0 A \tan \Lambda_{ac} \tag{26}$$

where a_0 is the wing section's lift-curve slope.

The second method is Kapteyn's empirical equation (Kapteyn, 1972; given in detail in Torenbeek, 1982) which is based on the lifting surface theory:

$$C_{m_{ac}} = C'_{m_{ac}} - \left(K_{\lambda,A} a_w A \tan \Lambda_\beta\right)\theta \tag{27}$$

where $\tan \Lambda_\beta = \tan(\Lambda/\beta)$

$$K_{\lambda,A} = 0.066 + 0.029\lambda - 0.03\lambda^2 + 0.00273(\lambda - 0.095)\beta A$$

and a_w is the wing's lift-curve slope. For this method,

$$K_0 = 1 \tag{28}$$

$$K_\theta = -K_{\lambda,A} a_w A \tan \Lambda_\beta \tag{29}$$

The third method is the widely used empirical equation from the USAF-DATCOM (Finck, 1978):

$$C_{m_{ac}} = K_0 C'_{m_{ac}} + K_\theta \theta \tag{30}$$

$$K_0 = \frac{A \cos^2 \Lambda}{A + 2\cos \Lambda} \tag{31}$$

$$K_\theta = \left(\frac{\Delta C_{m_F}}{\theta}\right) \tag{32}$$

No empirical expression for K_θ was given and charts for this parameter were provided for taper ratios of 0, 0.5, and 1 only.

Sample values of $C_{m_{ac}}$ given by equations (24), (27), and (30) are shown in Figure 12, along with values provided by our empirical law, equation (4). The results indicate that our law is in close agreement with Anderson's method (equation (24)) since the relative difference in $C_{m_{ac}}$ values between the two methods is less than 4%.

The agreement of Kapteyn's method (equation (27)) with our empirical law is less favorable than that of the method of Anderson. One reason for the discrepancy is that K_0 in equation (27) takes the value 1 regardless of aspect ratio, taper ratio, or sweep. This disagrees with both Anderson's method and our findings. For instance, the charts for constant E in equation (24) give values of K_0 as large as 1.16 (Abbott & Von Doenhoff, 1959) and this is larger by

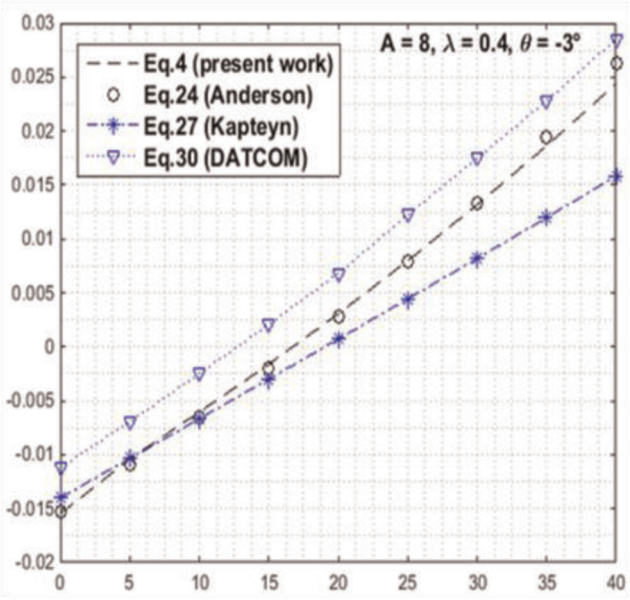

Figure 12. Comparison between $C_{m_{ac}}$ values given by our new empirical law and those given by equations (24), (27), and (30).

16%. Also, our values for K_0 vary from 1.11 for $A = 10$, $\Lambda = 0$, and $\lambda = 1$ down to about 0.85 for $A = 4$, $\Lambda = 40^\circ$, and $\lambda = 0.2$. The constant value of 1 assigned to K_0 in equation (27) is off by more than 10% for straight wings and as much as 15% for highly swept wings. The second reason is that, at large sweep angles, coefficient K_θ given by equation (29) deviates away from the values given by the other three methods (Figure 13).

The method of the USAF-DATCOM (equation (30)) is inaccurate for all values of the sweep angle as seen in Figure 12. The main problem with this equation is in K_0 and this is rather obvious if we look at its expression for straight wings, i.e., for $\Lambda = 0$:

$$K_0 = \frac{A}{A + 2} \tag{33}$$

Our method and the two methods discussed previously all agree that, for a straight tapered wing, K_0 is either exactly 1 for Kapteyn's method or greater than 1 for Anderson's method and our new empirical law. Equation (33), however, gives much lower values. If we consider an aspect ratio $A = 4$ for instance, then $K_0 = 0.67$. This is off by 33% with respect to the method of Kapteyn and by about 40% with respect to both Anderson's method and our

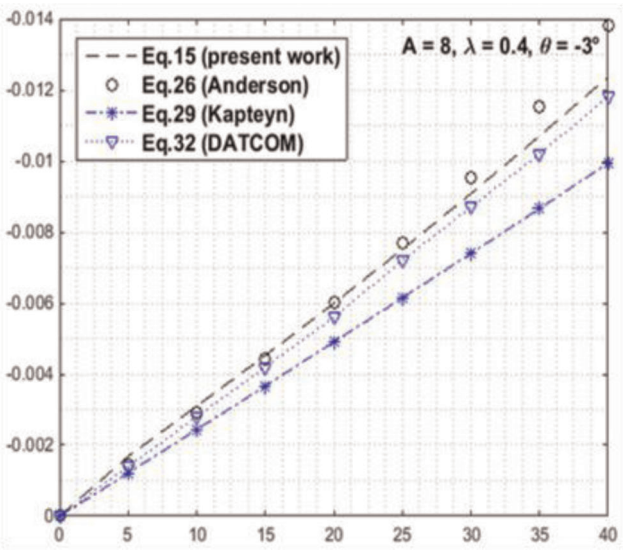

Figure 13. Comparison between the values of coefficient K_θ as given by the new empirical law and equations (24), (27), and (30).

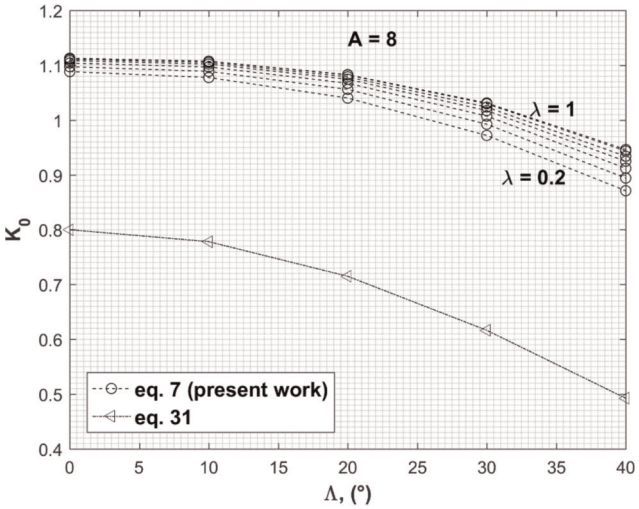

Figure 14. Variation of coefficient K_0 with the sweep angle for $A = 8$.

new empirical law. The discrepancy in K_0 increases with the sweep angle as indicated in Figure 14.

To illustrate this point further, we consider a wing with $A = 6$, $\lambda = 0.5$, $\theta = 0$, $\Lambda = 9.67°$, and the NACA 23012 airfoil (Pearson & Anderson, 1939). The experimental value for $C_{m_{ac}}$ is -0.014 while the one given by equation (30) is -0.01 and this is off by 29%. Our new empirical law gives a value of -0.015 and the difference is 7%. This is reasonably close to the test value.

Validation of the Compressibility Correction Law

The compressibility correction coefficient K_M given by our empirical law for the compressibility effect on $C_{m_{ac}}$ (equation (22)) was compared to values obtained from a chart based on experimental data given in the

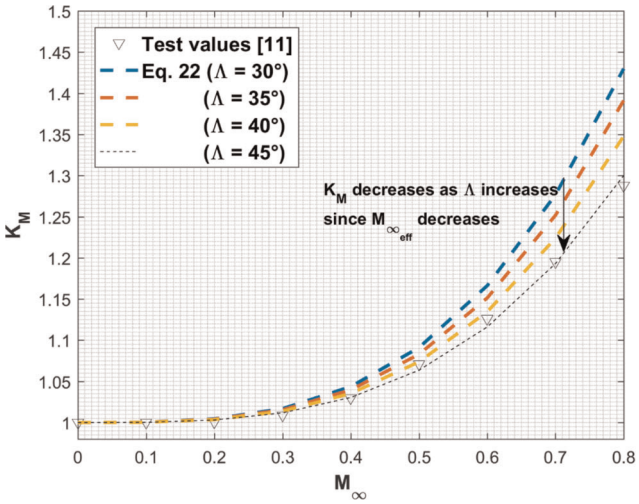

Figure 15. Equation (22) versus test values of K_M (Finck, 1978).

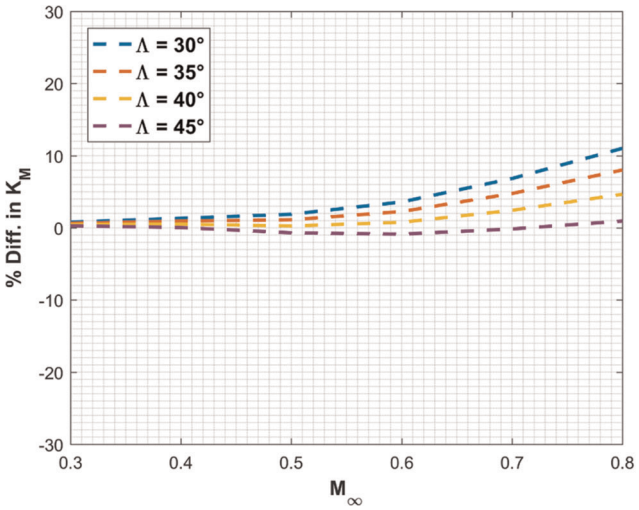

Figure 16. Percent differences between values of K_M given by equation (22) and test values.

USAF-DATCOM (Finck, 1978). Values from this chart are plotted in Figure 15, along with curves given by equation (22) for sweep angles of 30°, 35°, 40°, and 45°. The percent differences between our values and the test data from the DATCOM chart are shown in Figure 16.

There was no mention of any value of the sweep angle Λ in association with the USAF-DATCOM chart, as if K_M were independent of the wings' sweep. Our computations show that this is not the case, and this is physically justifiable since the aerodynamic behavior of swept wings is dictated by the component of the Mach number which is normal to a wing's leading edge. Or, this component decreases with sweep for a given free-stream Mach number. Since Figure 9 shows that K_M increases with the Mach number, it only makes sense that, for a given Mach number and as the sweep angle increases and the effective Mach number decreases, the compressibility correction factor K_M should decrease. This is in accordance with our

results shown in Figure 15 where, at a given free-stream Mach number, coefficient K_M decreases as the sweep angle goes from 30° to 45°.

The percent differences in K_M values between equation (22) and the test data from the chart generally increase with the Mach number. At Mach 0.8, the difference is less than 1% for a sweep angle of 45°, less than 4.7% for 40°, and less than 8% for 35°. Apparently, the test data from the USAF-DATCOM chart were obtained for high sweep angles.

Conclusions

A new empirical law for the prediction of the pitching moment coefficient at the aerodynamic center of trapezoidal wings with linear twist and constant taper and sweep was introduced. The data used in establishing this law were generated using the vortex-lattice method. The empirical law is quite general in that it does not rely on the use of charts and spans the full practical range of values of taper ratio, aspect ratio, and sweep angle for subsonic aircraft. It is, however, limited to positive sweep angles and does not accommodate the case of varying airfoils along the span. The empirical law was first derived for the incompressible regime and then, using Göthert's rule, more data were generated and used to establish an additional empirical law for the compressibility effect on the zero-lift pitching moment coefficient.

The results have been fairly well validated by comparison to some experimental values, the relative difference being typically around 5%. Our method was also compared to three pre-existing methods. Good agreement with the method of Anderson was obtained for all sweep angles, while the method of Kapteyn tends to be inaccurate at high sweep angles. It has also been shown that the widely referenced method from the USAF-DATCOM is highly inaccurate. This emphasizes the importance of our new empirical law which henceforth provides a reliable method for the prediction of this important parameter in the conceptual and preliminary stage of aircraft design. Another contribution of this work is the empirical law for the compressibility effect on the zero-lift pitching moment coefficient. The methods of Anderson and Kapteyn discussed in this work are limited to the incompressible regime. The USAF-DATCOM does not provide an empirical law for the compressibility effects but only gives a chart which does not account for the influence of wing sweep on the compressibility effect.

This work can be extended to include the case of forward swept wings, wings with variable airfoil along the span, and the effect of flaps on the zero-lift wing pitching moment coefficient.

References

Abbot, I. H., & Von Doenhoff, A. E. (1959). *Theory of wing sections*. Dover Publications.

Anderson, R. F. (1936). *Determination of the characteristics of tapered wings*. NACA Report No. 572.

Bertin, J. J., & Smith, M. L. (1998). *Aerodynamics for engineers* (3rd ed.). Prentice Hall.

Finck, R. D. (1978). *USAF stability and control DAT-COM*. Clayton, MO: Global Engineering Documents.

Kapteyn, P. (1972). *Design charts for the aerodynamic characteristics of straight and swept, tapered, twisted wings*. Delft University of Technology, Department of Aeronautical Engineering, M-180.

Multhopp, H. (1942). *Aerodynamics of fuselage*. NACA TM-1036.

Neely, R. H., Bollec, T. V., Westrick, G. C., & Graham, R. R. (1947). *Experimental and calculated characteristics of several NACA 44-series wings with aspect ratios of 8, 10, and 12, and taper ratios of 2.5 and 3.5*. NACA TN No. 1270.

Pearson, H. A., & Anderson, R. F. (1939). *Calculation of the aerodynamic characteristics of tapered wings with partial-span flaps*. NACA TR 665.

Roskam, J. (1979). *Airplane flight dynamics and automatic flight controls*. Roskam Aviation and Engineering Corporation.

Shapiro, A. (1952). *The dynamics and thermodynamics of compressible flow* (Vol. I). John Wiley & Sons, Inc.

Torenbeek, E. (1982). *Synthesis of subsonic aircraft design*. Delft University Press, Kluwer Academic Publishers.

Yahyaoui, M. (2014). Generalized vortex lattice method for predicting characteristics of wings with flap and aileron deflection. *International Journal of Mechanical, Aerospace, Industrial, and Mechatronics Engineering*, *8*(10), 1690–1698.

Yahyaoui, M. (2019a). A new method for the prediction of the downwash angle gradient. *International Journal of Aviation, Aeronautics, and Aerospace*, *8*(3/9).

Yahyaoui, M. (2019b). A comparative aerodynamic study of nonplanar wings. *International Journal of Aviation, Aeronautics, and Aerospace*, *6*(4/10).